Work function studies of rare-gas/noble metal adsorption systems using a Kelvin probe

C. Hückstädt, S. Schmidt,* and S. Hüfner
Universität des Saarlandes, Fachrichtung 7.2—Experimentalphysik, D-66041 Saarbrücken, Germany

F. Forster and F. Reinert
Universität Würzburg, Experimentelle Physik II, D-97074 Würzburg, Germany

M. Springborg
Universität des Saarlandes, Fachrichtung 8.1—Chemie, D-66041 Saarbrücken, Germany
(Received 5 October 2005; revised manuscript received 21 December 2005; published 6 February 2006)

We present a systematic study of the change in work function of noble metal (111) surfaces (Cu, Ag, Au) when being covered with a monolayer of a rare gas (Ar, Kr, Xe). Using a Kelvin probe the experiments show a decrease of the work function of the adsorbate covered system compared to the clean metal surface, in agreement with physisorption theory. The difference in work function depends both on the substrate and adsorbate being the highest for the Xe/Cu system and the lowest for Ar/Au. A comparison is performed with angle-resolved ultraviolet photoemission spectroscopy data using the binding energy shift of the (111) surface states of the same adsorbate/substrate systems, and with density functional calculations on simple model systems.

DOI: 10.1103/PhysRevB.73.075409 PACS number(s): 73.30.+y, 68.47.De, 73.20.At, 82.45.Mp

I. INTRODUCTION

Adsorption processes play an important role in various fields of surface science ranging from material sciences and pharmacy to biochemistry and nanotechnology. When investigating metal surfaces an important material-dependent parameter is the work function Φ, being very sensitive to crystallographic orientation, surface structure, and impurities.[1–4] Efforts in molecular electronics can only be successful if the molecule/metal interface is understood in detail.[5] Therefore the understanding of kinetics and topography of adsorbate systems[6–8] are of considerable significance. Rare-gas atom adsorption on noble metal surfaces can be regarded as the simplest model system for the study of adsorption processes and properties.[9–11] Both partners in this process have a very simple closed shell electronic structure (where the metals are lacking an electron). This fact, however, is also the challenge in the understanding of the adsorption process, because second order polarization processes play a dominant role. The interaction of a rare-gas atom with a noble metal surface consists of two terms: a repulsive Pauli interaction and an attractive van der Waals interaction.

A Kelvin probe is the most suitable tool for determining the work function, since it is nondestructive and not causing any desorption of even weakly bound adsorbates. Furthermore, it consists of a simple and inexpensive design, being easy to modify and having a good energy resolution in the meV range. The Kelvin method, improved by Zisman,[12] is based on few components: a capacitance (two different electrical conductors being connected externally) and a device (ampere meter) measuring the charge transfer (see Fig. 1).

Vibrating one of the plates of the capacitance (e.g., plate B in Fig. 1 is the oscillating plate and A represents the sample surface) produces an alternating current

$$I(t) = \frac{dQ(t)}{dt} = (V_b + V_{CPD})\frac{dC(t)}{dt}. \tag{1}$$

While V_b represents a potential applied externally, V_{CPD} arises from the contact potential difference (CPD) between the plates A and B. No current flows if

$$V_b = -V_{CPD}, \tag{2}$$

meaning that the related electric field between the plates is cancelled out and the CPD equals the work function difference between the materials A and B,

$$eV_{CPD} = -\Delta\Phi_{AB}, \tag{3}$$

with electron charge e. Adjusting V_b in order to get $I(t)=0$ leads to the desired work function difference. This method is realized using the sample as one plate and a reference electrode as the other; however, it measures an average work function of the sample area the size of the reference electrode and the relative value to the reference electrode only.

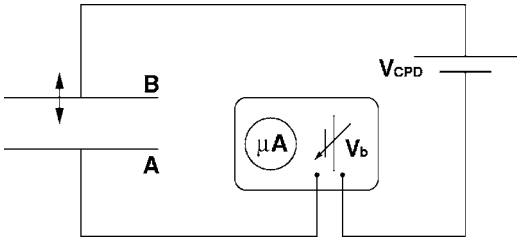

FIG. 1. Schematic diagram of the Kelvin method: two electrical conductors A and B form a capacitor, make up a contact potential difference (CPD). B is the oscillating plate of the capacitor while V_b stands for a potentiometer.

 ©2006 The American Physical Society

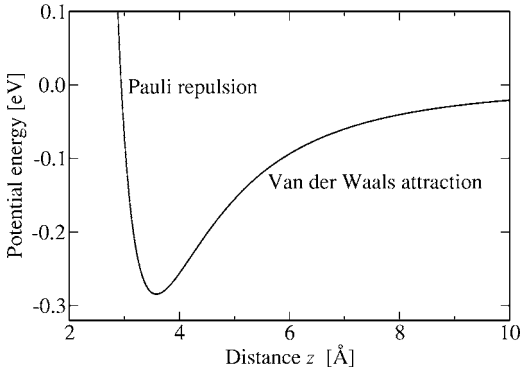

FIG. 2. Qualitative physisorption potential of Xe on Cu(111) as a function of the distance z from the metal surface.[19]

We investigated the work function differences of adsorbate systems, using the simple, prototypical model of one monolayer of a rare gas (Ar, Kr, Xe) on a (111) noble metal substrate (Cu, Ag, Au). Previous studies of the change in work function between the clean substrate and the adsorbate system had been performed on just a few combinations, namely for Xe on Ag(111)[13,14] and Xe on Cu(111)[14,15] using the method of photoelectron spectroscopy. Leatherman *et al.*[16] have studied one of the systems [Kr on Ag(111)] using the same experimental technique as used here. No systematic study of these adsorbate/substrate systems by work function difference measurements is available. Theoretical work function calculations using different models have been performed for the clean (111) substrates;[5,17,18] however, there are only a few calculations available on the adsorbate systems, e.g., such as for Xe on Cu(111) by Da Silva *et al.*[19] who applied density functional theory (DFT) calculations to additionally identify on-top sites for the Xe adatoms as the energetically most favorable position as verified in recent experiments[20] and for the other rare-gas/noble metal systems as well.[21]

The binding nature of these systems is physisorption, describing the weak bond between the closed valence electronic shell of the rare gas and the solid metal surface.[22,23] At low temperatures, a gas atom is physisorbed by the van der Waals interaction. When approaching the surface it becomes polarized and creates an image dipole inside the solid resulting in a dipole-dipole attraction. While this dispersion force dominates at long range, the so-called Pauli repulsion is characteristic for the physisorption potential at small distances close to the surface leading to an equilibrium spacing of 3.60Å for Xe on Cu[20] (see Fig. 2). The repulsive (short-range) interaction can be related to adsorbate induced shifts of the binding energy of Shockley-type surface states. The surface electronic structure influenced by the adsorbates was studied by Forster *et al.*[24] using angle-resolved ultraviolet photoemission spectroscopy (ARUPS) for exactly the same rare-gas/noble metal systems as in the present communication. Consequently, a comparison of the ARUPS results is possible with the results of this work function study since perturbations of the electronic structure by the Pauli repulsion are also assumed to be partly the reason behind the lowering of the work function by the interface dipoles.[5] All dipoles contribute to a change of the surface potential, meaning the greater the surface dipole moment, the greater the work function decrease which explains qualitatively the systematics of work function and surface state binding energy changes.

For clarity we have to note the following: The term "binding energy" has in the context of this paper two different meanings. It describes the energy with which a rare-gas atom is bound to a noble metal surface. Equally this term describes the energy of a surface state on a noble metal surface as measured by photoemission spectroscopy. Which of the two meanings is relevant is always clear from the context in which the term is used.

As we shall argue in this paper, the shifts of the orbital energies due to the rare-gas adsorption are not only due to electrostatic interactions (i.e., fluctuating dipole moments) but have contributions from the interactions of the wave functions of the adsorbants with those of the surface. Compared with those of "normal" chemical bonds, they are weak, but for the systems of the present study they become significant. By studying the work functions we can identify these electronic interactions.

Recently Da Silva *et al.*[25] have made a comprehensive theoretical [DFT + local density approximation (LDA) or generalised gradient approximation (GGA)] study of the adsorption of Xe on various metal surfaces, among them Cu(111). Their finding was (as argued intuitively with respect of Fig. 2), that the interaction between the Xe atom and the noble metal surface consists of a repulsive Pauli term and an attractive polarization (van der Waals) term, which, however, could also be interpreted as a chemical interaction between Xe and the metal surface. The bandwidths of the s, p, and d bands of the metal atoms in the topmost layer broaden as the Xe approaches the metal surface, which also holds for the Xe states. These changes could be taken as an indication of hybridization of adsorbate and metal states, such as occurs in covalentlike bonds. Da Silva *et al.*[25] calculate a change of the work function of Cu(111) if covered with a monolayer of Xe of 960 meV and 200 meV using the LDA or GGA approximation respectively, compared to the experimental value of 620 meV as reported in this paper. The different numbers obtained by the DFT-LDA and DFT-GGA methods indicate the accuracy with which such properties can be calculated reliably these days, whereby it shall be remembered that this difference first of all is due to differences in the optimized structure and only partly in the description of the electronic interactions. It also indicates that one is dealing with quite subtle effects. The calculated adsorption energy for Xe on Cu(111) is 277 meV (LDA) and 40 meV (GGA) compared to the experimental value[20] of 187 meV, indicating again that while theory is able to determine the right order of magnitude for such a property it struggles with the determination of the exact magnitude.

II. EXPERIMENTAL SETUP, METHOD OF WORK FUNCTION DETERMINATION, AND SAMPLE PREPARATION

For the experiments we used a Kelvin probe Typ S by Besocke Delta Phi, Jülich/Germany[26] which was placed into the setup of a SCIENTA SES-200 UHV chamber[27] with a

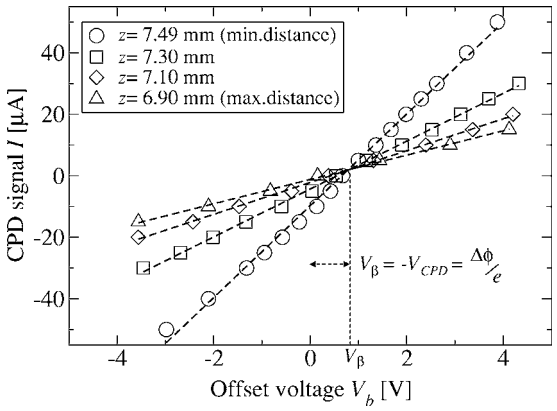

FIG. 3. Method to determine a relative work function value of Cu(111) at 300 K: For different probe-sample distances z (relative height of the manipulator) the curves $I(V_b)$ intersect on β, V_β corresponds to the CPD and work function value.

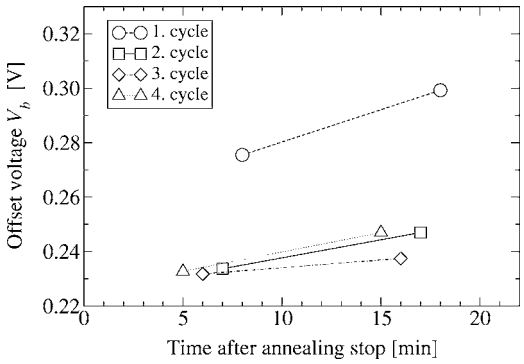

FIG. 4. Work function measurements on Ag(111) at 300 K after consecutive sputtering-annealing cycles with 40 min time interval between the cycles.

base pressure of $\approx 5\times 10^{-11}$ mbars. A manipulator, connected to a closed-cycle refrigerator, serves to move the sample to either the work function or the low-energy electron diffraction (LEED) measurement position. The reference electrode represents the oscillating capacitance, consisting of an inert Au grid 2.5 mm in diameter and piezoelectrically driven at a resonance frequency of ≈180 Hz. Shielding of the two electrical feedthrough wires was applied, while the probe comes with shielding itself to avoid the influence of stray capacitances.[8,28–30] Spurious effects to the CPD signal could be minimized by a rigid mounting of probe and wires. The Kelvin control 07 electronic device by Besocke Delta Phi not only optimizes the signal-to-noise ratio of the CPD signal[31] but also controls all relevant probe settings. Drawn from the reference electrode the ac component of the CPD signal is amplified, rectified by a phase sensitive detector (PSD), which gives a dc signal to be integrated, superimposed by the offset voltage and applied as compensation voltage to the reference electrode. Ranging from −5 V to 5 V the offset voltage V_b can be adjusted manually to null the CPD signal.

Since there are still stray effects contributing to the signal, the offset potential does not exactly match the true work function. Therefore we plotted offset voltages V_b versus the corresponding CPD signal I for different probe-sample distances (≈0.5−2 mm). The curves $I(V_b)$ intersect on a point β being unequal to zero due to stray capacitances. V_β matches the true work function difference between the surfaces of reference electrode and sample[3,29,32,33] (see Fig. 3). In order to shorten this procedure we took data from two distances and six different offset voltages only, which did not affect the coordinates of V_β. However, setting and scale reading together took about 2 min time and resulted in one work function value.

The substrate samples are commercially available polished (111) single crystals, which were prepared *in situ* by repeated sputtering-annealing cycles to obtain a clean and well-ordered surface. Proof for that is observed surface states after applying the identical preparation procedure to the same samples at the same SCIENTA instrument.[34,35] However, no subsequent work function/surface state measurements were performed; in addition, LEED measurements showed a good single crystal surface for each material.

Work function measurements following each preparation cycle also give evidence of the cleanliness of the substrate as shown in Fig. 4. From the second cycle on, the work function remains constant at room temperature and for 40 min time intervals between cycles.

If the sample is transferred onto the cooled manipulator directly after preparation one gets unstable work function results due to residual gases being dissolved out of the manipulator by the heated sample and instantly being adsorbed on the sample surface. To avoid this effect, a 13 min cooling down interval was necessary. At temperatures below 60 K an adsorption of residual gases lowers the work function of the clean substrate surface with time. So once the sample is on the measuring position, adsorbate gas is filled into the chamber at a partial pressure of $\approx 1\times 10^{-7}$ mbars until the adsorbate monolayer is formed, monitored by simultaneous LEED investigation. Care had to be exercised such that the electron beam of the LEED gun did not destroy the adsorption layer. This was easy for Xe, possible for Kr, and very difficult for Ar, for which only a check after the work function measurements was possible. The critical adsorption temperature is ≈60 K for Xe, 38 K for Kr, and 25 K for Ar. Work function measurements were performed right after the adsorbate layer formation as well as 5, 10, 20, and 30 min later. The adsorption conditions were always chosen so, that only one monolayer of adsorption took place.[36,37]

III. EXPERIMENTAL RESULTS

As an example for an adsorbate/substrate system we present data of Xe/Cu(111) in Figs. 5 and 6. The squares in Fig. 5 stand for the clean Cu(111) sample; however, due to the adsorption of residual gases, the values at 55 K and 60 K (single squares in Fig. 5) are lowered with respect to the stable data set at room temperature (connected squares). Compared to the Xe/Cu(111) values (circles) there is a significant difference in the work function, being constant for a time of 30 min. Such as in this case for Xe/Cu(111), the work function of all adsorbate/substrate systems is lowered with respect to the clean (111) substrates upon noble gas adsorption.

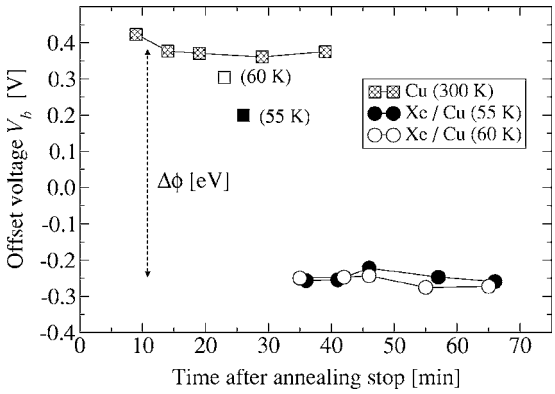

FIG. 5. Work function change between clean Cu(111) at 300 K and the commensurable Xe/Cu(111) superstructure at 55 K and 60 K. The single squares (open square 60 K, filled square 55 K) represent work function measurements of the clean Cu(111) sample at the given low temperatures. The diminished offset voltage of the clean surface at 55 and 60 K is most likely produced by residual gas. Although the data of the clean (low-temperature) surfaces show some scatter, such a scatter is not observed in the data from the Xe covered surfaces.

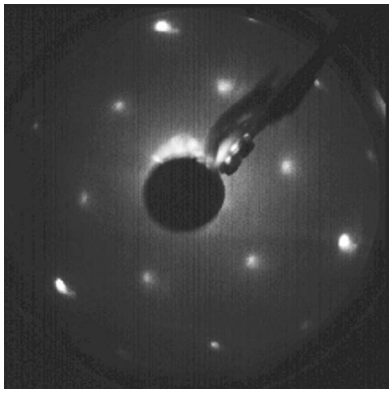

FIG. 6. LEED pattern at 60 K for the $(\sqrt{3}\times\sqrt{3})R30°$ Xe/Cu(111) lattice (E_0=135 V).

Xenon adsorbs on Cu(111) as a commensurable $(\sqrt{3}\times\sqrt{3})R30°$ lattice at on-top sites.[19,21] The LEED image (Fig. 6) shows six inner spots forming a hexagon which correspond to the xenon superstructure. This lattice structure is rotated by 30° with respect to the Cu(111) substrate pattern formed by the outer spots with the typical threefold symmetry.[21] Being the only commensurate system of all systems under investigation here, there is no hint that this specific structure influences the work function in a particular way, when comparing the results of work function changes with all the other incommensurate systems.

Table I summarizes the results of the measurements of work function change. The mean value of the five to six data points of each measurement set is calculated, both for the clean substrate and different sets of the adsorbate covered system. The difference $\Delta\Phi$ is shown in Fig. 7 and had to be corrected due to a systematic error (equal to a factor of 0.95) of the offset-voltage indicator. Its setting accuracy of ±5 mV limits the precision of calculating the work function data and therefore limits the energy resolution. All sets of work function measurements resulted in work function data being constant for a long period of time (up to 85 min after annealing stop) at various temperatures with the small deviations only, as given in Table I.

IV. DISCUSSION

The values of all work function differences corresponding to the same adsorbate/substrate system are displayed in Fig. 7 taken from Table I. Obviously, there is an ordering of data with respect to the choice of adsorbate/substrate combination. Repeated measurements show a high reproducibility (Table I). The substrate coverage with an adsorbate monolayer always lowers its work function, the difference $\Delta\Phi$ getting larger from Au to Ag to Cu and also from Ar to Kr to Xe. This order correlates with the decreasing atomic number of the noble metal substrates and an increasing atomic number of the rare-gas adsorbates. Both trends stand for a decreasing nobleness. Consequently, Ar/Au(111) results in the least work function change and Xe/Cu(111) in the largest of all systems investigated.

Due to the highest polarizability of all three rare gases under investigation, Xe develops the strongest dipole layer and surface potential when being adsorbed, and is therefore most strongly bound to the metal surface. Thus, Xe produces the largest work function drop $\Delta\Phi$, and its interaction forces are the largest with Cu, the least noble substrate metal. A correlation between adsorption energy, dipole moment, and work function change was demonstrated for Xe/Cu(111) and Xe/Ag(111)[38] and will be valid for the other adsorbate/substrate systems as well. Photoelectron spectroscopy data of

TABLE I. Measured work function difference $\Delta\Phi$[eV] between the surfaces of rare-gas adsorbate/noble metal substrate systems and corresponding clean noble metal substrates.

	Adsorbate		
Substrate	Ar	Kr	Xe
Au(111)	0.35±0.02	0.41±0.04	0.53±0.02
	0.40±0.03	0.43±0.02	0.52±0.02
average	0.38±0.03	0.42±0.02	0.53±0.03
Ag(111)	0.41±0.03	0.45±0.01	0.59±0.04
	0.39±0.04	0.45±0.03	0.61±0.03
	0.39±0.02	0.46±0.02	0.57±0.04
		0.48±0.02	
average	0.40±0.03	0.46±0.02	0.59±0.03
Cu(111)	0.42±0.04	0.48±0.02	0.61±0.05
	0.37±0.03	0.47±0.03	0.60±0.03
	0.38±0.02	0.51±0.04	0.63±0.04
	0.44±0.02	0.49±0.04	0.64±0.04
	0.44±0.03		
	0.45±0.03		
average	0.42±0.03	0.49±0.03	0.62±0.03

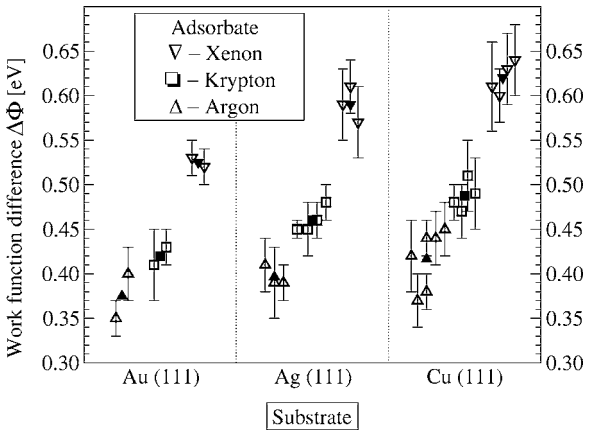

FIG. 7. Graphical overview of the data from Table I. Full symbols are the mean values taken from the measuring series of a particular adsorbate/substrate system.

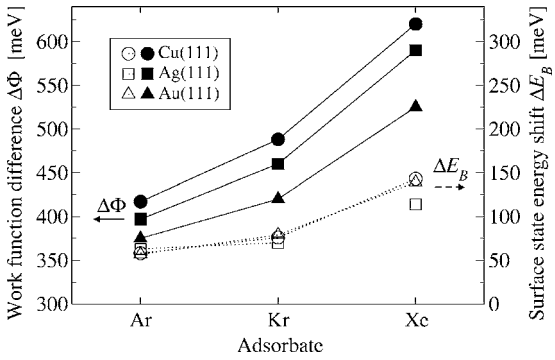

FIG. 8. Data of work function measurements $\Delta\Phi$[meV] (mean values taken from Fig. 7) and measurements of the surface state binding energy shift ΔE_B[meV] by Forster *et al.* at $T=30$ K (Ref. 24), both data sets are of the same adsorbate/substrate systems. The ΔE_B data point for Xe on Ag(111) is taken from an STM measurement by Hövel *et al.* at $T=5$ K (Ref. 39).

the work function lowering, e.g., for Xe/Cu(111) (0.58 eV,[14] 0.5 eV[15]) are in agreement with our mean value of 0.62 eV. As shown in the graphical overview of Fig. 7, the work function data of Xe/Cu(111) match the systematics although this system shows a commensurate Xe superstructure.

To get further insight into the electronic properties of these adsorbate covered systems, we compare our work function data with the data of binding energy shifts of the (111) surface states collected on the same systems by Forster *et al.*[24] Figure 8 compares both data sets on a similar energy scale. While the work function change $\Delta\Phi$ depends as well on the adsorbate as on the substrate, the shift ΔE_B of the Shockley-type surface states towards the Fermi level[15,22] is almost independent of the substrate and is larger the higher the atomic number of the adsorbate.

At this point a more general comment seems to be in order. The comparison between the changes in work function and that of the surface state energies is not trivial, because these energies contain different contributions. The work function [in a simple approximation, see Eq. (4)] contains two contributions, namely the difference in total energy between the initial (E_N) and final (E_{N-1}) state and a polarization term. The latter one is—in terms of the picture provided by density functional theory—a function of the electron density. This is determined by the atomic and solid state properties of the materials and in this sense also by the surface dipole layer. However, the comparison in Fig. 8 indicates that the changes induced by the rare gases are more dependent on the substrate metal for the work function than for the surface state energies. This is not unreasonable. The surface state is localized with its wave function mostly in the surface layer (decaying exponentially into the vacuum), and on this length scale the change in electronic structure induced by an adsorbate is dominated by its properties. On the other hand the work function is determined by a long range interaction (decaying as $1/z^3$ into the vacuum) and this is also determined by the specific metal substrate.[40] This qualitative reasoning makes the different behavior of the work function changes and the surface state energy changes as displayed in Fig. 8 understandable.

What we want to aim at by the comparison in Fig. 8 and also by others in this section is to find out what kind of correlation exists between different surface properties of the (111) surfaces of noble metals upon coverage with rare gases. These trends we hope can stimulate further theoretical analysis and thereby lead to a deeper understanding of the phenomena of rare-gas adsorption on noble metals and their influence on the surface properties.

These general considerations can be quantified somewhat with the numbers in Table II for Xe on the noble metal surfaces and Table III where additional numbers are compiled.

In a simple approximation the work function of a material is given by[42]

$$\Phi = D - \bar{\mu}, \tag{4}$$

where D is a surface polarization term and $-\bar{\mu}$ the so-called internal work function. Here $\bar{\mu}$ is the chemical potential and is defined as

TABLE II. Absolute (and normalized) data for the Xe on Au(111), Ag(111) and Cu(111): work function change $\Delta\Phi$ (this work), surface state energy change ΔE_{SS} (Ref. 24), calculated Xe polarization energy (Ref. 41) and Xe adsorption energy (Ref. 41); in each column also the values normalized to that of Xe on Au(111) (norm) are given for easier comparison.

Substrate, Xe on:	$\Delta\Phi$(eV)	norm	ΔE_{SS}(eV)	norm	$-V_{pol}$(eV)	norm	Xe-ads. energy (eV)	norm
Au(111)	0.53	1.00	0.14	1.00	0.34	1.00	0.20	1.00
Ag(111)	0.59	1.11	0.11	0.81	0.32	0.94	0.30	1.50
Cu(111)	0.62	1.17	0.14	1.00	0.27	0.79	0.23	1.15

TABLE III. Surface state energy change ΔE_{SS} (Ref. 24), adsorption energy $\Delta E_{ads.}$ (Refs. 36 and 37), work function change $\Delta\Phi$, c coefficient in the $c/(z-z_0)^3$ term of the potential used for the work function calculations (Ref. 41) and polarization energy (Ref. 41) for noble metal/rare-gas systems.

Adsorbate	Substrate	ΔE_{SS} (eV)	$\Delta E_{ads.}$ (eV/atom)	$\Delta\Phi$ (eV)	c coeff.	$-V_{pol}$ (eV)
	Au	0.139		0.53	0.88	0.34
Xe	Ag	0.114	0.225	0.59	0.81	0.32
	Cu	0.143		0.62	0.77	0.27
	Au	0.079		0.42	0.61	–
Kr	Ag	0.070	0.151	0.46	0.56	–
	Cu	0.076		0.49	0.52	–
	Au	0.057		0.38	0.44	–
Ar	Ag	0.063	0.99	0.40	0.40	–
	Cu	0.058		0.42	0.37	–

$$\bar{\mu} = E_{N-1} - E_N, \tag{5}$$

namely, the difference in the total ground state energies of the sample in the N-electron state and with one electron removed. D is a dipole layer term. It represents the fact that at the surface the electrons spill out into the vacuum leaving behind a layer of positive charge leading to a dipole layer at the surface; in addition D contains a term which originates from the smoothing out of the electron density at the surface. In first order it is the change of this dipole layer by an adsorbate, which leads to a work function change by an adsorbate, and one can therefore write (approximately)

$$\Delta\Phi = \Delta D. \tag{6}$$

Now the interaction between an adsorbate and a surface has as mentioned two terms. First there is a long-range attractive van der Waals term[41]

$$V_{pol}(z) = -\frac{c}{(z-z_0)^3}, \tag{7}$$

where z_0 is the distance of the so called reference plane with respect to the surface (defined as the position of the top most atomic layer) and is the mathematical surface position. The position of the adsorbed atom above the surface (z_{eq}) is large compared to z_0. The second repulsive term in the adatom-surface interaction comes from the overlap of the wave functions of the two systems and reflects the Pauli repulsion. In order to keep the discussion as simple as possible, we will assume in a first approximation that z_0 and z_{eq} are the same for all noble metal/rare-gas combinations (note this setting is only a rough approximation and serves to detect the trends in the data presented here). Then, the parameter c is a measure of the polarization energy, produced by the rare gases and for that reason it is listed in Table III. We emphasize that through these simple considerations, we introduce some uncertainty into our estimates, and that more system-specific considerations will improve the accuracy of our estimates.

TABLE IV. Noble metals: averaged rare-gas-induced changes of the surface state energy ΔE_{SS}, the rare-gas-induced work function changes ($\Delta\Phi$), the c parameter in the polarization term $[\propto c/(z-z_0)^3]$, and polarizability of the rare gases (Ref. 43); also given are the values normalized to those of the noble metal surfaces covered by Xe.

Adsorbate	ΔE_{SS}(eV)	$\Delta\Phi$(eV)	c coeff.	polarizability
Xe	0.132/1	0.58/1	0.82/1	27/1
Kr	0.074/0.56	0.46/0.79	0.56/0.68	17/0.63
Ar	0.059/0.45	0.40/0.69	0.39/0.48	11/0.41

It is not unreasonable to assume in view of the systematics evident from Table III that the main effect in the rare-gas-induced electronic changes comes from the polarizability of the rare-gas atom. To make this evident we have compiled in Table IV the surface state shift, the work function shift induced by the rare-gas adsorption, and the c parameters (averaged for the three noble metals) for each rare gas and compared them with their polarizabilities.

In order to make this comparison more transparent in each case, again the normalized numbers relative to the rare gas Xe are given. These normalized numbers show a remarkable consistent trend for all the properties, where only the work function changes $\Delta\Phi$ show a less pronounced dependence on the rare gases, than the surface state energy and the c parameter. We can only speculate why this is so. The c parameter (van der Waals coupling strength) should scale closely with the polarizability because the van der Waals coupling is given in first order by the polarizability. The connection of the polarizability with the surface state energy shift is obvious. One can assume[9] that since the move of the surface state closer to the Fermi energy means a charge depletion of this state, this depleted charge goes into unpopulated states of the adsorbate. This charge redistribution is calculated in the DFT calculations which are discussed below. The unpopulated states are, on the other hand, a measure of the polarizability, which makes this correlation at least understandable. With respect to the correlation of the work function change with the polarizability, one would at first hand assume a very strong correlation because the polarizability gives the magnitude of the additional dipole moment, which in turn gives the change of the work function. However it was pointed out already that while ΔE_{SS} depends on the short-range (exponentially decaying) charge density of the substrate, $\Delta\Phi$ depends on the $1/z^3$ term in the van der Waals interaction, making the numbers in Table IV intuitively understandable.

In summary, the change of the work function of the (111) surface of the noble metals upon coverage with rare gases has been measured. The magnitude of the shift scales with increasing polarizability of the rare gas (Ar, Kr, Xe) and with decreasing nobleness of the substrate (Au, Ag, Cu). The data qualitatively correlate with the change of surface state energies, and the c coefficient of the attractive van der Waals potential $[c/(z-z_0)^3]$ of the rare-gas–noble metal system. In the following two sections more quantitative considerations for the noble metal–rare-gas interaction will be presented.

A. Atomic orbital energies

To study the interactions between the rare gases and the noble metals in more detail, we performed parameter-free calculations on the simplest possible systems, i.e., the diatomic *M*-*G* molecules with *M* being Cu, Ag or Au and *G* being Ar, Kr, or Xe. We used a full-potential, density functional method that is based on expanding the eigenfunctions to the Kohn-Sham equations in a basis set of linearized muffin-tin orbitals, as described in details elsewhere (see, e.g., Refs. 44 and 45). Since we also study heavier atoms we included all relativistic effects, also spin-orbit couplings. In describing exchange- and correlation-effects we used a local density approximation, which is known to lead to too strong interatomic interactions, whereas electronic orbitals and their energies usually are accurately described. Since our aim is to study the latter, and not to optimize the geometry of the system, we consider this approximation fully justified.

We considered four different interatomic distances for each of the nine *M*-*G* systems, corresponding to interatomic distances of 16, 8, 7, and 6 a.u. (1 a.u.$\approx$0.53 Å). The first value is so large that it approximates the infinite separation, whereas the other ones are expected to describe realistic metal-gas interatomic distances as they are found for the rare-gas atoms on the surface. Referring to Fig. 2, we mention that with the density functional calculations we will first of all obtain an accurate description of the electronic interactions (i.e., the Pauli repulsion) and not of the van der Waals attraction. But as the figure indicates, the equilibrium geometry is one for which the two types of interactions are in balance. Moreover, the work function is first of all an electronic property so that a study of the electronic properties as function of (realistic values of) the gas-metal interatomic distances should be optimal for the present purpose. Due to the well-known deficiencies of density functional calculations in describing accurately van der Waals interactions, we shall not try to calculate the equilibrium *M*-*G* interatomic distances, although the results of Kirchner *et al.*[46] on Ar/Ag(111) suggest that at least this system can be described accurately with current density functional methods and that the simplest possible systems give precise information on the electronic interactions, which is very important for the present work.

Before discussing the results we stress that the results cannot yield an accurate reproduction of the experimental results. Reducing both the semi-infinite metal crystal and the layer of gas atoms to single atoms is indeed a severe approximation. On the other hand, since the metal consists of only one type of (metal) atoms, suggesting that the orbitals have significant resemblance with those of the atoms and are not obscured by charge-transfer effects or the formation of covalent bonds, and since, moreover, the gas atoms are only weakly interacting, we will expect that the electronic interactions are dominated by those of the individual atoms; there is, e.g., no charge-transfer effects. Thus, although we consider a highly simplified model system, we expect that it will catch the trends of the experimental observations. Support for this is given by the work of Kirchner *et al.*[46] who showed that the electronic properties of Ar/Ag(111) were accurately reproduced with even the simplest possible model systems like the Ar-Ag diatomic system.

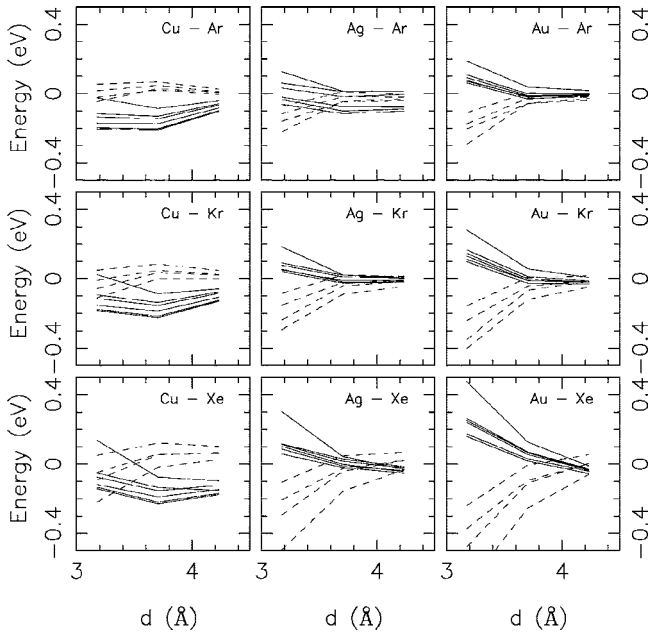

FIG. 9. The variation in the orbital energies for the nine *M*-*G* diatomic systems as found in the density-functional calculations. Dashed (solid) lines represent orbitals on the gas (metal) atoms.

For the well-separated metal and gas atoms, the valence orbitals split into low-lying *s* and *p* orbitals from the gas atoms and higher lying *d*- and *s*-valence orbitals from the metal atoms. These lie at roughly −25 eV and −11 eV for the gas-atom orbitals, essentially independent of whether we consider Ar, Kr, or Xe. The valence orbitals of the metals lie above those of the rare gas atoms, i.e., at −4 eV to −5 eV for Cu, at −4 eV to −7 eV for Ag, and at −6 to −10 eV for Au. Since we consider finite systems, we have here used an energy scale with the energy zero put at the position where the electrons are infinitely far apart with regard to the systems of interest.

In Fig. 9 we show the results of the calculations, i.e., the changes in the orbital energies compared to those of the "infinite" separation. The full curves refer to the orbitals on the metal atoms, and the dashed ones to the orbitals on the gas atoms.

For the largest separation (i.e., 8 a.u.$\approx$4.24 Å), most of the orbitals lower their energy compared to the infinite separation. In this range the orbitals are mainly influenced by the mutual polarization of the two atoms, although it is weak. Decreasing the interatomic distance, the electronic orbitals of the two atoms start to interact. Since the orbitals for the Au atom have energies closest to those of the gas atoms, perturbation theory gives that these orbitals will interact strongest with the orbitals of the gas atoms, whereas the same argument gives that the interactions between the orbitals of Cu atoms and those of the gas atoms will be weakest. This is, indeed, confirmed by the data in Fig. 9. A further result of this analysis is that new orbitals will be formed for each pair of orbitals, one from the metal atom (at higher energy) and one from the gas atom (at a lower energy). One is a bonding combination with an even lower energy than the energy of the gas-atom orbital with its major support from the gas atom

as well as an antibonding combination with an even higher energy than that of the metal orbital and with its major support from the metal atom. In this picture, the metal orbitals will increase their energies, in accord with the experimental results.

The electronic-structure calculations confirm the existence of orbital interactions (although fairly small) at the smallest interatomic distances. This interpretation together with the results given in Fig. 9 suggest that the shifts for Xe as an adsorbate will be the largest and those for Ar the smallest. This can be rationalized through the higher polarizability of Xe or, equivalently, through the larger number of unoccupied orbitals for Xe at relatively low energies. This finding is confirmed by the experimental results.

Cu shows the largest shifts and Au the smallest ones for all rare gases. Therefore, it may be suggested that the *M*-*G* separations are smallest for $M=$Cu and largest for $M=$Au.

B. Mulliken overlap populations

The concept of Mulliken populations allows for a qualitative description of interatomic interactions. It is closely linked to the way electronic-structure calculations are performed, most notably to the fact that any electronic orbital is expanded in a set of basis functions. For the Mulliken populations, it is important that the basis functions are atom centered.

Accordingly, we write

$$\psi_i(\vec{r}) = \sum_p \sum_l \sum_\alpha c_{ipl\alpha}\chi_{pl\alpha}(\vec{r}), \tag{8}$$

where ψ_i is the ith orbital and $\chi_{pl\alpha}$ is a basis function centered on atom p, having an angular dependence given through l, and having any other dependence (e.g., the m quantum number, or a specific radial dependence) as specified through α. Notice that in our theoretical approach the basis functions are dynamically adapted to the potential of the complete system although they preserve their angular character. Since the ψ_i are normalized we have

$$1 = \langle\psi_i|\psi_i\rangle = \sum_{p_1,p_2}\sum_{l_1,l_2}\sum_{\alpha_1,\alpha_2} c^*_{ip_1l_1\alpha_1}c_{ip_2l_2\alpha_2}\langle\chi_{p_1l_1\alpha_1}|\chi_{p_2l_2\alpha_2}\rangle$$

$$= \sum_{p_1,p_2}\sum_{l_1,l_2} n_{ip_1p_2l_1l_2} \tag{9}$$

$$= \sum_{p_1,p_2} n_{ip_1p_2}. \tag{10}$$

Through the last identity [Eq. (10)], the orbital has been split into *on-site* ($p_1=p_2$; also called *net*) and *overlap* ($p_1 \neq p_2$) populations. We shall here concentrate on the latter. If $n_{ip_1p_2}>0$, the overlap between the basis functions from the p_1th and from the p_2th atom is constructive for the ith orbital, i.e., there is an overall bonding interaction. Equivalently, $n_{ip_1p_2}<0$ if the interaction is antibonding. Thus, the overlap populations provide a quantitative measure for the covalency between the atoms.

More detailed information is obtained from the penultimate identity above [Eq. (9)], where the interactions are split into l-specific components. Thus, for the systems of our interest we can distinguish between, e.g., the interactions between the gas s or p functions and the metal s or d functions. In this way, it is possible to analyze the individual contributions from the different types of functions.

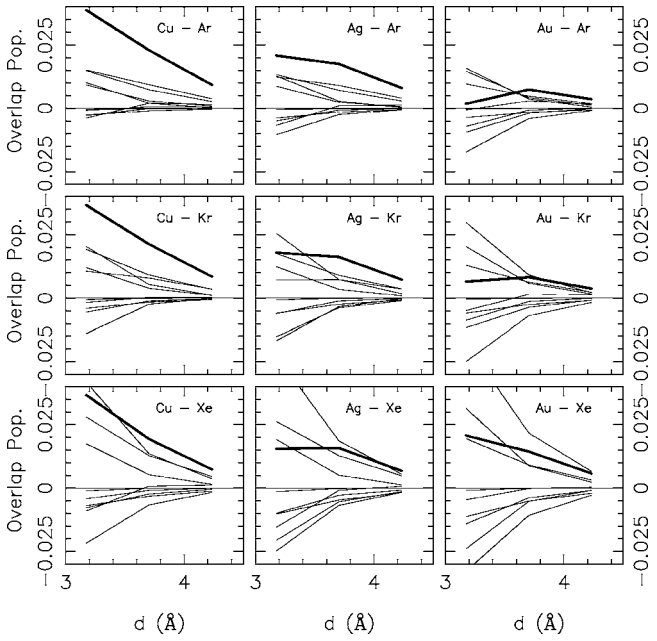

FIG. 10. The variation in the Mulliken overlap populations for the nine *M*-*G* diatomic systems as found in the density functional calculations. In each panel, the thin curves show the nine l-decomposed overlap populations $N_{p_1p_2l_1l_2}$ [Eq. (11)], whereas the thick curve shows their sum $N_{p_1p_2}$ [see Eq. (12)].

Finally, by adding all contributions from all occupied orbitals we obtain the quantities that are displayed in Fig. 10,

$$N_{p_1p_2l_1l_2} = \sum_{i=1}^{\text{occ}} n_{ip_1p_2l_1l_2}, \tag{11}$$

$$N_{p_1p_2} = \sum_{i=1}^{\text{occ}} n_{ip_1p_2}. \tag{12}$$

The overlap populations are not measurable quantities and should not be overinterpreted. The most important information is that overlap populations different from zero indicate the existence of covalent interactions between the atoms. Thus, the fact that we find many non-negligible overlap populations (when decomposing them into different l components) suggests that the interactions between the orbitals of the different atoms are complicated.

The importance of the electronic orbital interactions between metal and gas is illustrated in Fig. 10. This figure shows the Mulliken overlap population between the metal and the gas atoms for the same structures as in Fig. 9. That is, for each system and structure we study the overlap of the valence (s, p, or d) basis functions of the metal atom with the overlap of the valence (s, p, or d) basis functions of the gas atom for all occupied orbitals. This gives in total nine different l-decomposed overlap populations and their sum is the

total overlap population between the two atoms. The *s* and *p* functions of the gas atoms as well as the *s* and *d* functions of the metal atoms are those contributing the most to the total overlap population. These functions possess different decay behaviors far away from the nuclei, implying that also the individual overlap populations decay differently, which is clearly recognized in the figure. This has the consequence that the total overlap population, being the sum of the differently decaying contributions (that even may have different signs), possesses a quite complicated behavior, most clearly seen for the Au-Xe system.

For Cu most overlap populations are positive suggesting that Cu-*G* (*G* being a rare-gas atom) interactions are stronger bonding than is the case for the other metals. Therefore, the orbital shifts for the Cu-based systems are the largest ones, as observed in experiment. However, the fact that the orbital shifts are smallest for the Au-based systems does not imply that the orbital interactions for those are weakest, but rather that there are many interactions of both signs that add to a smaller sum.

We stress that the overlap populations are not the electronic energies. However, they are useful in quantifying the orbital interactions between the metal atoms and the gas atoms. Although they are small, they are non-negligible. Finally, in Fig. 11 we show the radial parts of the valence orbitals for the isolated atoms as obtained numerically within density functional theory. The spatial extensions of the valence *s* and *p* orbitals for the rare-gas atoms are very similar implying that both types of orbitals will interact with those of other atoms when the interatomic distances are sufficiently small. Moreover, it is also seen that the rare-gas atom orbitals are more compact than those of the noble metal atoms. For the latter, mainly the *s* orbitals extend far away from the nuclei, but for the heavier atoms also the *d* functions are so delocalized that when bringing the metal and the gas atoms into a 3–4 Å distance, there will be interactions between all types of valence orbitals.

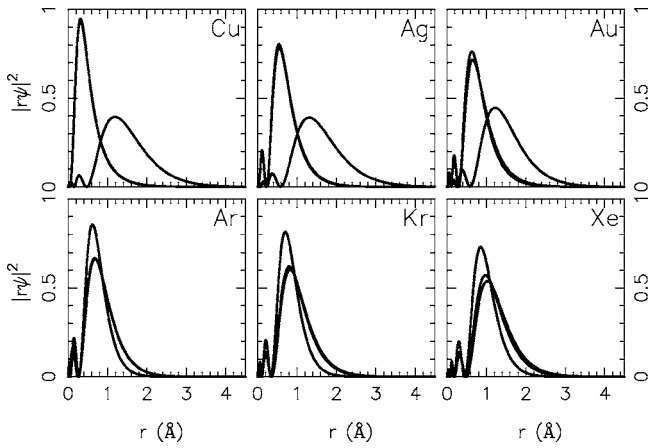

FIG. 11. The radial parts of the square of the wave functions for the valence orbitals of the isolated atoms. For the rare-gas atoms, we show the *s*- and *p*-valence orbitals, and for the noble-metal atoms the *s*- and *d*-valence orbitals. Since relativistic effects have been included, two *p* and *d* functions are shown; most clearly recognizable for the heavier elements.

V. CONCLUSIONS

In this work we have studied the work function change of the (111) surfaces of the noble metals if covered with rare gases. The work functions are reduced upon rare-gas coverage, and the reductions show a systematic trend being largest for Xe and smallest for Ar—which suggests a correlation of the changes with the polarizabilities of the rare-gas atoms. In order to get more insight into this problem, we have studied the electronic orbitals of the surface of a nobel metal, in particular when it is covered with a rare gas. The fact that the orbital energies change upon rare-gas adsorption gives indication of non-negligible interactions, although the experiments cannot directly reveal their nature. One type of interactions is the van der Waals interaction, which has been studied in detail theoretically by, e.g., Zaremba and Kohn.[41] Then, the surface and the rare-gas atoms will polarize each other mutually, ultimately leading to additional potentials that are felt by the electrons. Although a qualitative agreement with the experimentally measured work functions could be obtained, a quantitative description was not provided. Therefore, we studied also extremely small model systems with density functional calculations, i.e., two-atomic systems. We found that orbital interactions are non-negligible, and that even several different types of valence orbitals interact, leading to a complex gas-metal system that hardly can be quantified through simple models. Thus, we have to conclude that the van der Waals interaction is only one part of the interaction between noble metals and rare gases.

ACKNOWLEDGEMENTS

This work was supported by the Deutsche Forschungsgemeinschaft directly and through the SFB 277.

*Corresponding author. E-mail address: sw.schmidt@mx.uni-saarland.de

[1] K. Wandelt, Appl. Surf. Sci. **111**, 1 (1997).
[2] I. D. Baikie and P. J. Estrup, Rev. Sci. Instrum. **69**, 3902 (1998).
[3] I. D. Baikie, P. J. S. Smith, D. M. Porterfield, and P. J. Estrup, Rev. Sci. Instrum. **70**, 1842 (1999).
[4] K. Germanova, C. Hardalov, V. Strashilov, and B. Georgiev, J. Phys. E **20**, 273 (1987).
[5] P. S. Bagus, V. Staemmler, and C. Wöll, Phys. Rev. Lett. **89**, 096104 (2002).
[6] S. C. Fain, L. V. Corbin, and J. M. McDavid, Rev. Sci. Instrum. **47**, 345 (1976).
[7] H. A. Engelhardt, P. Feulner, H. Pfnür, and D. Menzel, J. Phys. E **10**, 1133 (1977).
[8] J. S. W. deBoer, H. J. Krusemeyer, and N. C. B. Jaspers, Rev. Sci. Instrum. **44**, 1003 (1973).
[9] L. Bruch, M. W. Cole, and E. Zaremba, *Physical Adsorption: Forces and Phenomena*, Intl. Series Monographs in Chemistry,

No. 33 (Oxford University Press, 1997), chap. 6.2, pp. 227–239.
[10] M.-C. Desjonquères and D. Spanjaard, *Concepts in Surface Science* (Springer, New York, 1995).
[11] G. Vidali, G. Ihm, H.-Y. Kim, and M. W. Cole, Surf. Sci. Rep. **12**, 135 (1991).
[12] W. A. Zisman, Rev. Sci. Instrum. **3**, 367 (1932).
[13] R. J. Behm, C. R. Brundle, and K. Wandelt, J. Chem. Phys. **85**, 1061 (1986).
[14] S. Eder, K. Markert, A. Jablonski, and K. Wandelt, Ber. Bunsenges. Phys. Chem. **90**, 225 (1986).
[15] M. Wolf, E. Knoesel, and T. Hertel, Phys. Rev. B **54**, R5295 (1996).
[16] G. S. Leatherman and R. D. Diehl, Surf. Sci. **380**, 455 (1997).
[17] N. D. Lang and W. Kohn, Phys. Rev. B **3**, 1215 (1971).
[18] C. J. Fall, N. Binggeli, and A. Baldereschi, Phys. Rev. B **61**, 8489 (2000).
[19] J. L. F. Da Silva, C. Stampfl, and M. Scheffler, Phys. Rev. Lett. **90**, 066104 (2003).
[20] T. Seyller, M. Caragiu, R. D. Diehl, P. Kaukasoina, and M. Lindroos, Chem. Phys. Lett. **291**, 567 (1998).
[21] R. D. Diehl, T. Seyller, M. Caragiu, G. S. Leathermann, N. Ferralis, K. Pussi, P. Kaukasoina, and M. Lindroos, J. Phys.: Condens. Matter **16**, S2839 (2004).
[22] N. Memmel, Surf. Sci. Rep. **32**, 91 (1998).
[23] E. Bertel and N. Memmel, Appl. Phys. A **63**, 523 (1996).
[24] F. Forster, S. Hüfner, and F. Reinert, J. Phys. Chem. B **108**, 14692 (2004).
[25] J. L. F. Da Silva, C. Stampfl, and M. Scheffler, Phys. Rev. B **72**, 075424 (2005).
[26] K. Besocke and S. Berger, Rev. Sci. Instrum. **47**, 840 (1976).
[27] T. Finteis, Ph.D. thesis, Universität des Saarlandes, Saarbrücken, 1999.
[28] B. Ritty, F. Wachtel, R. Manquenouille, F. Ott, and J. B. Donnet, J. Phys. E **15**, 310 (1982).
[29] L. B. Harris and J. Fiasson, J. Phys. E **17**, 788 (1984).
[30] N. A. Surplice and R. J. D'Arcy, J. Phys. E **3**, 477 (1970).
[31] I. D. Baikie, S. Mackenzie, P. J. Z. Estrup, and J. A. Meyer, Rev. Sci. Instrum. **62**, 1326 (1991).
[32] J. Bonnet, L. Soonckindt, and L. Lassabatre, Vacuum **34**, 693 (1984).
[33] H. Baumgärtner and H. D. Liess, Rev. Sci. Instrum. **59**, 802 (1988).
[34] F. Forster, G. Nicolay, F. Reinert, D. Ehm, S. Schmidt, and S. Hüfner, Surf. Sci. **532–535**, 160 (2003).
[35] G. Nicolay, F. Reinert, F. Forster, D. Ehm, S. Schmidt, B. Eltner, and S. Hüfner, Surf. Sci. **543**, 47 (2003).
[36] J. Unguris, L. W. Bruch, E. R. Moog, and M. B. Webb, Surf. Sci. **87**, 415 (1979).
[37] J. Unguris, L. W. Bruch, E. R. Moog, and M. B. Webb, Surf. Sci. **109**, 522 (1981).
[38] A. Jablonski, S. Eder, K. Markert, and K. Wandelt, J. Vac. Sci. Technol. A **4**, 1510 (1986).
[39] H. Hövel, B. Grimm, and B. Reihl, Surf. Sci. **477**, 43 (2001).
[40] There has been a lively discussion whether the work function is basically determined by the simple long-range interaction (Refs. 47 and 48) ($\propto 1/z^3$) or if a more complex description might be necessary to obtain quantitative results, especially for the induced moment and/or atomic susceptibility in terms of the polarizability α (Refs. 49 and 50). Also in the discussion led by Flynn *et al.* (Ref. 51) and Lang *et al.* (Ref. 52) some questions still remained open.
[41] E. Zaremba and W. Kohn, Phys. Rev. B **13**, 2270 (1976).
[42] *Photoemission in Solids I*, edited by M. Cardona and L. Ley, vol. 26 of *Topics in Applied Physics* (Springer-Verlag, Berlin, 1978).
[43] G. Reisfeld and U. Asaf, Phys. Rev. A **49**, 348 (1994).
[44] M. Springborg and O. K. Andersen, J. Chem. Phys. **87**, 7125 (1987).
[45] M. Springborg, J.-L. Calais, O. Goscinski, and L. A. Eriksson, Phys. Rev. B **44**, 12713 (1991).
[46] E. J. J. Kirchner, A. W. Kleyn, and E. J. Baerends, J. Chem. Phys. **101**, 9155 (1994).
[47] P. R. Antoniewicz, Phys. Rev. Lett. **32**, 1424 (1974).
[48] P. R. Antoniewicz, Surf. Sci. **52**, 703 (1975).
[49] R. A. Kromhout and B. Linder, J. Chem. Phys. **81**, 2516 (1984).
[50] B. Linder and R. A. Kromhout, J. Phys. Chem. A **107**, 3270 (2003).
[51] C. P. Flynn and Y. C. Chen, Phys. Rev. Lett. **46**, 447 (1981).
[52] N. D. Lang, A. R. Williams, F. J. Himpsel, B. Reihl, and D. E. Eastman, Phys. Rev. B **26**, 1728 (1982).